PAPER

How cellulose particles influence streamer propagation and branching in transformer oil: a 2D modelling perspective

View the article online for updates and enhancements.

Plasma Research Express

PAPER

How cellulose particles influence streamer propagation and branching in transformer oil: a 2D modelling perspective

Yuan Li[1] , Yahong Li, Jiaye Wen , Linbo Li, Luning Wang and Guanjun Zhang[1]

State Key Laboratory of Electrical Insulation and Power Equipment, Xi'an Jiaotong University, Xi'an 710049, People's Republic of China
[1] Authors to whom any correspondence should be addressed.

E-mail: liyuan8490@xjtu.edu.cn and gjzhang@xjtu.edu.cn

Abstract

The streamer discharges and electric breakdown in insulating liquid like transformer oil are undesirable for power equipment. However, the physical processes of streamer propagation and branching events in dense liquid dielectrics are not well understood. In this paper, we develop an improved fluid model to investigate the interactions of cellulose particles with streamer propagation and branching behaviors. We elaborately select the number of cellulose particles (single or multiple particles), their size and locations to elucidate the influencing mechanisms. The simulation results show that when the heads of streamer contact with the surface of the cellulose particle, the local electric field increases sharply, hence the rise of ionization rate and velocity. The scattering electric field lines guide the streamer head away from the surface, thereby causing branching to occur. The interactions between the two split streamers allow one head to continuously propagate, while the other dies out due to insufficient ionization rate. When the particle is too small or too far away to the streamer channel, it has no pronounced impact on the streamer propagation. While placing the particle very close to or on the route of discharge channel will cause the streamer to creep on the cellulose particle and to branch more.

1. Introduction

Transformer oil is a kind of excellent liquid dielectrics for great electric breakdown strength, heat-conducting, and self-healing properties [1]. It has been widely used in various power equipment, such as power transformers [2], pulsed power devices [3], high voltage reactors [4]. In these high voltage devices, insulating oil usually plays such a function in combination with insulating paper to form oil-paper immersed insulation system [5]. The electrical behaviours subjected to high electric field and the possible breakdown phenomena have been of great practical interest [3].

The events leading to breakdown in oil immersed insulation are usually denoted as streamers, including all types of discharge channels, like slow bushy or tree type and fast filamentary type [6, 7]. Streamers initiate where the local electrical field is strongest and rapidly penetrate into non-ionized regions due to the electric field enhancement in the front of streamer heads [8]. They usually take place prior to a total breakdown which is undesirable under growing requirements for safe operation of high voltage equipment of modern power system [9]. Hence, the phenomenon of streamers and the mechanisms behind have attracted intensive attentions from both scientific communities and industrial fields [10].

Branching phenomenon, as one of the most obvious features during streamer propagation, is observed in most streamer discharges, which may be due to local instability [11, 12], infinitesimal perturbation [13], electric field uniformity [14], additives [15], etc. Phenomenologically, streamers in gaseous atmosphere and dense liquid dielectric share similar structures, such as filamentary channels and multi-branches [16]. Streamer branching in gas is usually regarded as the result of Laplacian instability [11, 17] that occurs at the leading edge of a streamer, e.g. uncertainty of photo-ionization [18] and randomly scattered seed electrons [19]. However, the physical

processes during streamer initiation and propagation in dense liquid dielectrics are much less understood than in gaseous mediums [20]. This is because that the chemical composition of liquids is often more complex and until now we lack of experimentally microscopic parameters, e.g. electron drifting velocity.

Impact ionization, a key mechanism interpreting physical processes of streamers in gases, is not the predominating mechanisms responsible for the streamer initiation due to high rates of scattering and low mean free paths in dense liquid with high purity [21, 22]. While Zener ionization [23], usually describing the tunneling of electrons from the valence band to the conduction band in solids, is a frequently used theory in quantitatively elucidating the charged particles generation in dense liquid dielectric [21, 24]. However, we should remind that the electric parameters of liquid molecules used in the models, e.g. electron/ion mobilities, ionization potential of liquid molecules [24, 25], are obtained by simplified derivations, but not on a strong physical basis. The investigations by Aljure *et al* [26, 27] indicate that the Zener ionization model using the parameters from [24] may cause misestimation of the conduction currents after validating with the experimental current-voltage characteristics. For positive streamer discharge, the measured conduction current is well matched the Zener molecular ionization model under high electric field. However, they find that negative currents are much underestimated with Zener ionization mechanism, therefore they introduce impact ionization as an additional charge generation mechanism of negative streamers in mineral oil. In this manner, it is suggested Zener molecular ionization is dominant for positive polarity, while impact ionization prevails for negative streamers by Zener ionization providing initial seed of electrons.

It is worth noting that many experimental results highlight the complexity of breakdown phenomena in liquids [12, 21, 28]. Intensive studies propose that the variations of streamer properties significantly depend on the transition of propagation modes which are characterized by the travelling velocity [15]. For streamers of moderate velocity in non-polar liquids (e.g. ~1 to 3 km s^{-1}, i.e. the 2nd mode streamers), the development of a gaseous filament is a key procedure to explain propagation. While for those faster 3rd mode streamers (>10 km s^{-1}), Zener ionization, requiring higher local fields, may tentatively explain the propagation transitions [15].

Very recently, Madshaven *et al* [29] propose that radiation from the streamer head in dielectric liquid can cause photoionization, although the photoionization may work locally in space. Therefore, the physical mechanism of streamer propagation and branching in dense liquid may differ from that in gas and is more complicated but with insufficient knowledge to explain.

Streamer branching in liquid dielectrics may originate from impurities [30] existing in the vicinity of a streamer channel. It has been demonstrated that impurities may come from the conductive and insulation materials, e.g. the debris of insulating paper [1]. Impurities are regarded responsible for major discharge-related faults [31]. Previous investigation results [32–34] point out that streamer discharges are influenced by impurities and inhomogeneities within the oil through modifying the local electric field or disturbing the propagation path. Experimental observations show that the velocity and advancing direction of the streamers in air vary after interacting with the liquid droplets [32, 33] or liquid surface [35]. It is found that dielectric or conducting particles could guide the advancing direction of streamers [34]. In transformer oil, the correlation between impurities and branching indicates that advancing velocity and number of branches are mutually determined. For instance, it has been observed that streamers with low speed have more branches, and vice versa [36]. However, experimental recognition of branching is of difficulty in counting the number and measuring the length of branches, therefore it is very hard to achieve a comprehensive understanding of the streamer progress at the current experimental level.

Simulation of the branching behavior is also a very challenging task [28, 37]. Until recently, studies on the simulation of the branching behavior of both positive and negative streamers in gases have been reported [13, 37]. However, for liquid medium like transformer oil, very few computational investigations have addressed the branching behaviors. Aka-Ngnui [38] and Fowler [39] proposed fractal theory models to reproduce the branching progress, but these methods are based on a mathematical probability model instead of a physical manner. Jouya *et al* [24] developed a streamer branching model in transformer oil considering the charge carrier density fluctuations. They pointed out that branching is dependent on streamer head stability and inhomogeneity scale.

Physically, external microscopic impurities [40], originating from dielectric debris (mainly from cellulose particles of oil-paper insulation system), metal particles, gas bubbles etc, are also important sources triggering the branching in transformer oil. However, up to now, the influences of solid dielectric impurities like tiny cellulose particles on streamer branching are rarely discussed and less understood.

In this paper, we develop an improved fluid model to investigate branching behaviors of the fast propagation streamer (3rd mode) based on our previous work [41, 42]. The main improvements of this work are that we incorporate solid dielectric impurities (i.e. cellulose particles in our cases) in the model and investigate the interactions of particles with streamer propagation and branching behaviors. The crucial parameters

characterizing the discharge behaviors such as temporal-spatial evolutions of electric field, ionization rate and space charges are presented under varying conditions.

Specifically, this paper is organized as follows. Hydrodynamic model of charged particles is given in section 2 to describe physical processes of streamer discharges. We present the explicit simulation results of influences of cellulose particles on streamer propagation and branching in section 3, including circumstances with single impurity, multiple impurities, the size and their locations. Summaries and Conclusions are drawn accordingly in section 4.

2. Description of physical models

We employ a 2D fluid model in local field approximation to depict the generation, drift and recombination processes of charged particles, which are believed to play key roles in explaining discharge mechanisms in liquid dielectrics. Three continuity equations of carrier (1)–(3) and Poisson's equation (4) are coupled to account for the movement, generation and loss of electrons, positive and negative ions. The basic governing equations in transformer oil are given as

$$\frac{\partial \rho_p}{\partial t} + \nabla \cdot (\rho_p \mu_p \boldsymbol{E}_l) = G_I(|\boldsymbol{E}_l|) + \frac{\rho_p \rho_e R_{pe}}{e} + \frac{\rho_p \rho_n R_{pn}}{e} \tag{1}$$

$$\frac{\partial \rho_n}{\partial t} - \nabla \cdot (\rho_n \mu_n \boldsymbol{E}_l) = \frac{\rho_e}{\tau_a} - \frac{\rho_p \rho_n R_{pn}}{e} \tag{2}$$

$$\frac{\partial \rho_e}{\partial t} - \nabla \cdot (\rho_e \mu_e \boldsymbol{E}_l) = -G_I(|\boldsymbol{E}_l|) - \frac{\rho_p \rho_e R_{pe}}{e} - \frac{\rho_e}{\tau_a} \tag{3}$$

$$\nabla \cdot (-\varepsilon_l \nabla \varphi_l) = \rho_p + \rho_e + \rho_n \tag{4}$$

where e is electronic charge (1.6×10^{-19} C), ε_l the oil relative permittivity (2.2), φ_l the electric potential. $\boldsymbol{E}_l$ denotes the local electric field in transformer oil. ρ_p, ρ_e, and ρ_n are the densities of the positive ions, negative ions and electrons, while μ_p, μ_n, and μ_e are the mobilities of corresponding particles. R_{pn} and R_{pe} are the recombination coefficients for ion-ion and ion-electron; τ_a is the time constant of electron attachment.

On the generation source of charged particles, we employ a direct ionization of oil molecules by the action of the high electric field to interpret the mechanism of positive streamers. This mechanism is also known as Zener breakdown which has been originally responsible for the breakdown in solid dielectrics [21, 23], as it is given as

$$G_I(|\boldsymbol{E}_l|) = \frac{e^2 n_0 a |\boldsymbol{E}_l|}{h} \exp\left(-\frac{\pi^2 m^* a IP(|\boldsymbol{E}_l|)^2}{e h^2 |\boldsymbol{E}_l|}\right) \tag{5}$$

where h is Planck constant, a the molecular separation distance, m the effective electron mass, n_0 the density of ionizable molecule. $IP(|\boldsymbol{E}_l|)$ is the liquid-phase ionization potential as a function of the local electric field [43]. Other parameters used in the model can refer to our previous work [41, 42]. It should be added here that parameters used in (5) are derived from publications [24, 25] and they are not fully known and physically reliable based on the current knowledge.

For solid dielectric impurities, the dusts of tiny cellulose paper are considered. Note that in this circumstance, governing functions are required to modify. The conductivity of cellulose particles is reportedly less than 10^{-13} $\Omega^{-1}{\cdot}m^{-1}$, that is three orders lower than the conductivity of transformer oil (over 10^{-10} $\Omega^{-1}{\cdot}m^{-1}$). Therefore, the effect of conductivity on the movement of charged particles inside the cellulose particles in the nanosecond time scale is negligibly small. Here we set the conductivity of cellulose paper impurities as zero ($\sigma = 0$), which means that there is no space charge inside the impurities. The governing equations within solid dielectric impurities can be given as,
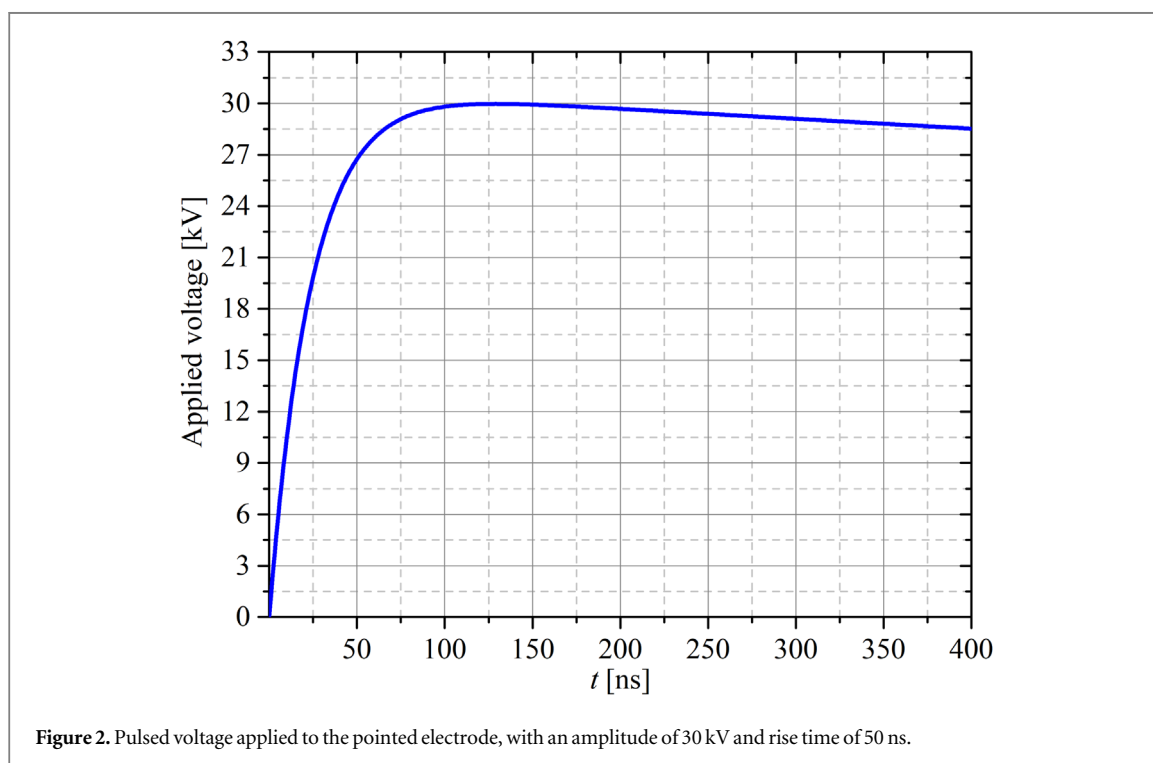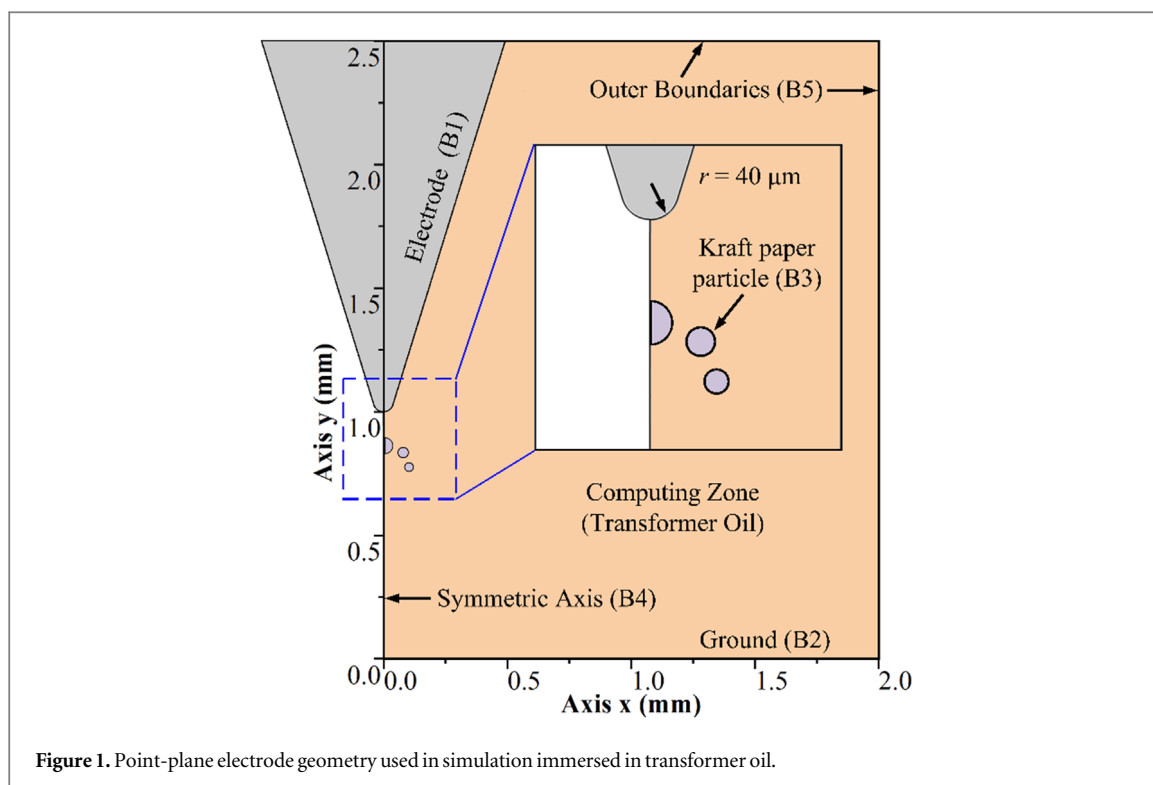
$$-\nabla \cdot (\nabla \varphi_s) = 0 \tag{6}$$

$$\boldsymbol{E}_s = -\nabla \varphi_s \tag{7}$$

where $\boldsymbol{E}_s$ and φ_s are the local electric field and electric potential within the solid dielectric impurities, respectively. As in the solid dielectric only displacement current exists, the surface charges on the solid-liquid interface is governed by

$$\frac{\partial \rho_s}{\partial t} = \boldsymbol{n} \cdot (\rho_n \mu_n + \rho_p \mu_p + \rho_e \mu_e) \boldsymbol{E}_s \tag{8}$$

$$\rho_s = \boldsymbol{n} \cdot (\varepsilon_s \boldsymbol{E}_s - \varepsilon_l \boldsymbol{E}_l) \tag{9}$$

where ρ_s and ε_s are the surface charge density and the relative permittivity of the solid dielectric impurities (4.4 for cellulose paper), respectively.

Figure 1. Point-plane electrode geometry used in simulation immersed in transformer oil.

Figure 2. Pulsed voltage applied to the pointed electrode, with an amplitude of 30 kV and rise time of 50 ns.

The geometry of the point-plane is shown in figure 1. The curvature radius of the pointed electrode is 40 μm and the gap spacing is 1 mm. We simplify the cellulose surface as an ideal sphere for faster modeling and computation although the surface of cellulose particle is rough and the shape will not be perfect spherical [44]. According to figure 1, boundaries are divided into five groups: B1 (Electrode), B2 (Ground), B3 (Impurity), B4 (Symmetry Axis), and B5 (Outer Boundaries). The boundaries for the carrier continuity equations on the B1 and B2 is out-flow, which means there only exists convection flux on the electrode (as the diffusion flux is zero). B5 is set no flux boundaries, indicating that there is no charged particle passing through. On the surface of impurity, the boundary conditions of B3 are given as [45],

$$n \cdot j_{\mathrm{p}} = \begin{cases} n \cdot j_{\mathrm{p}}, & n \cdot E \geqslant 0 \\ 0, & n \cdot E < 0 \end{cases} \tag{10}$$

$$n \cdot j_{\mathrm{n}} = \begin{cases} n \cdot j_{\mathrm{n}}, & n \cdot E \geqslant 0 \\ 0, & n \cdot E < 0 \end{cases} \tag{11}$$

$$n \cdot j_{\mathrm{e}} = \begin{cases} n \cdot j_{\mathrm{e}}, & n \cdot E < 0 \\ 0, & n \cdot E \geqslant 0 \end{cases} \tag{12}$$

where $j_{\mathrm{p}} = \rho_{\mathrm{p}}\mu_{\mathrm{p}}E$, $j_{\mathrm{n}} = \rho_{\mathrm{n}}\mu_{\mathrm{n}}E$ and $j_{\mathrm{e}} = \rho_{\mathrm{e}}\mu_{\mathrm{e}}E$ are the flux vector of positive ions, negative ions and electrons, respectively.

In this paper, the presented model and analysis of results concentrate on the streamer initiation and interactions of streamer head on the interface of liquid-solid dielectrics, hence the plasma inside the discharge channels are not highlighted. We neglect the gaseous nature of streamers in the modelling due to the fact that the most intense electron generation is occurred at the streamer head, and ignoring the vaporization of transformer oil behind the streamer head will not influence the maximum electric field at the streamer head. However, it is worth a mention that ignoring the vaporization of transformer oil may cause some errors in the extension and velocity of the streamer [46].

For Poisson equation (4), B1 and B2 are set potential boundaries: a pulsed voltage with an amplitude of 30 kV and rise time of 50 ns for B1, as shown in figure 2; 0 for B2. The boundary condition applied to B5 is zero charge condition for norm electric field along the boundaries is zero ($-n \cdot E = 0$).

3. Results and discussion

3.1. Single cellulose particle

We place a cellulose particle of 50 μm in diameter centered on the symmetric axis, 125 μm away from the tip of anode electrode. The typical temporal-spatial evolution of streamer propagation interaction with a cellulose impurity is shown in figure 3. When the streamer head propagates forward and approaches the micro-impurity at 41.6 ns, the maximum electric field increases dramatically from about 3.0×10^8 V m^{-1} to over 6.85×10^8 V m^{-1} (see Panel 3b). This is caused by an abrupt change of permittivity between oil ($\varepsilon_{\mathrm{l}} = 2.2$) and cellulose particle ($\varepsilon_{\mathrm{s}} = 4.4$), which is subject to the boundary continuity of the electric displacement D on the impurity surface, i.e., $\varepsilon_{\mathrm{l}}E_{\mathrm{l}} = \varepsilon_{\mathrm{s}}E_{\mathrm{s}}$. The electric field then decreases substantially when the streamer creeps along the surface of the cellulose particle (compare Panels 3c and 3d). After a short propagation, the streamer travels away from the dielectric surface but the field decreases continuously.

We calculate the velocity of streamer by estimating the propagating distance per time step. The fast increase of electric field accelerates the propagation of streamer. The propagating velocity, roughly 44.8 km s^{-1} shortly after the streamer head leaves away from the tip (Panel 3a), dramatically rises to 84.1 km s^{-1} before approaching the cellulose particle (Panel 3b). After contacting with the cellulose particle, the streamer adheres to the cellulose particle and creeps along the interface. However, the cellulose particle is, in fact, a barrier against the streamer head propagation, so that the velocity of the streamer slows down to 49.1 km s^{-1} along the interface (Panels 3c to 3d) and gradually decreases to 24.9 km s^{-1} before detaching from the dielectric particle (Panel 3e). As the streamer leaves the particle surface, the speed drops further to 9.1 km s^{-1} (Panel 3f).

Quantitatively, we draw the distribution of the electric field along the symmetric axis and along the arc of spherical surface of cellulose as shown in figure 4. The peak of electric field marks the location of the streamer head at 41.2 ns where $z = 72$ μm (see Panel 4a). Nevertheless, when the streamer head reaches the interface and propagates along the cellulose particle at 41.6 ns, the electric field on the symmetric axis does not show a similar ionization front as the typical streamer modeling in pure liquid and gases [47, 48]; it forms two field peaks. The locations of two peaks correspond to the upper edge and the lower edge of the streamer channel on the surface, and the distance between two edges determines the width of thin plasma layer ($\sim$5 μm). Note that the field on the lower edge (on the interface) is highly strong as 3.5×10^8 V·m^{-1}.

However, the electric field along the symmetric axis drops fast at 41.8 ns as the streamer head starts to creep along the cellulose surface and moves apart from the axis. Consequently, a substantially rise (up to 6.2×10^8 V·m^{-1}) in the field along the arc of the spherical surface is observed (see Panel 4b) at the same time. During the propagation, some of the positive ions are dispersed and attached to the surface cellulose particle, which reduce the density of space charge and hence the field at 42.0 ns. When the streamer head leaves the surface, the electric field clearly decreases to 2.5×10^8 V·m^{-1}.

Space charges, as a result of charge separation, play a dominate role in the formation of positive streamers in liquid by enhancing the field in front of the streamer head and hence guiding the further ionization. We plot the density distribution of space charge in figure 5 to explain a series of changes in maximum electric field, in which the time instants correspond to the situations of figure 3. The maximum space charge density appears at the
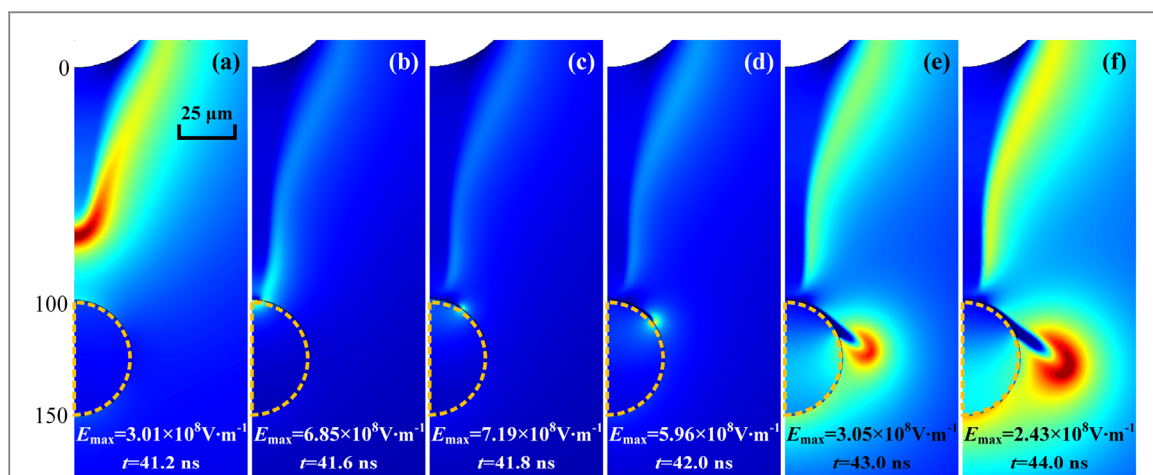
Figure 3. Electric field evolution of the streamer propagating and interacting with a cellulose particle of 50 μm in diameter (dotted half circle). The maximum electric field, E_{max}, is located by peak function imbedded in post-processing unit of COMSOL Multiphyics.
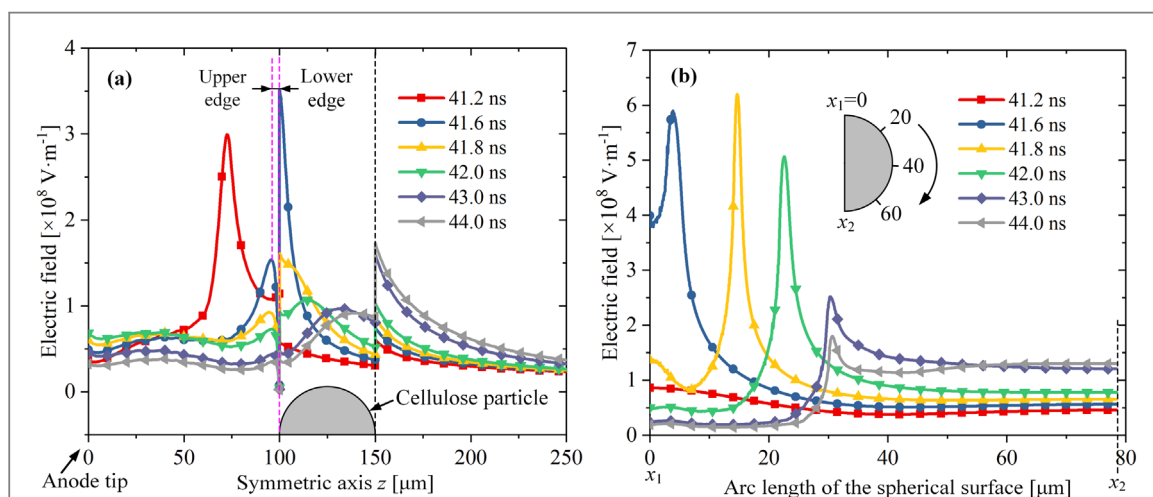

Figure 4. Electric field at different instants of time (a) along the symmetric axis and (b) along the arc of the cellulose particle surface. Note that the streamer reaches the cellulose particle at around 41.6 ns and travels away at around 43 ns. In panel (a), the gap between the upper and lower edges determines the width of thin plasma layer with very low field when the streamer just contacts the cellulose surface and propagates aside.
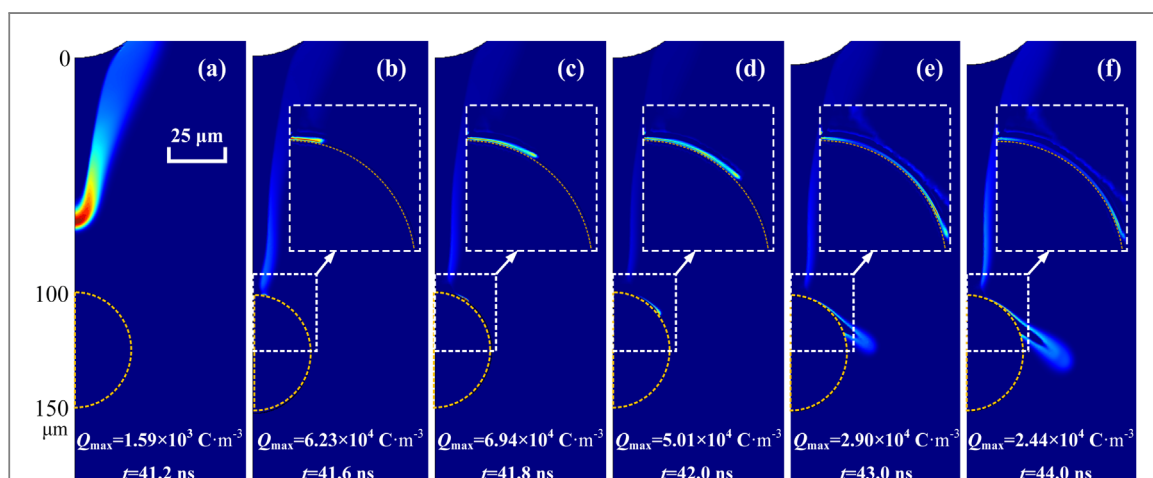

Figure 5. Space charge density evolution. The time instants are corresponding to that in figure 3.
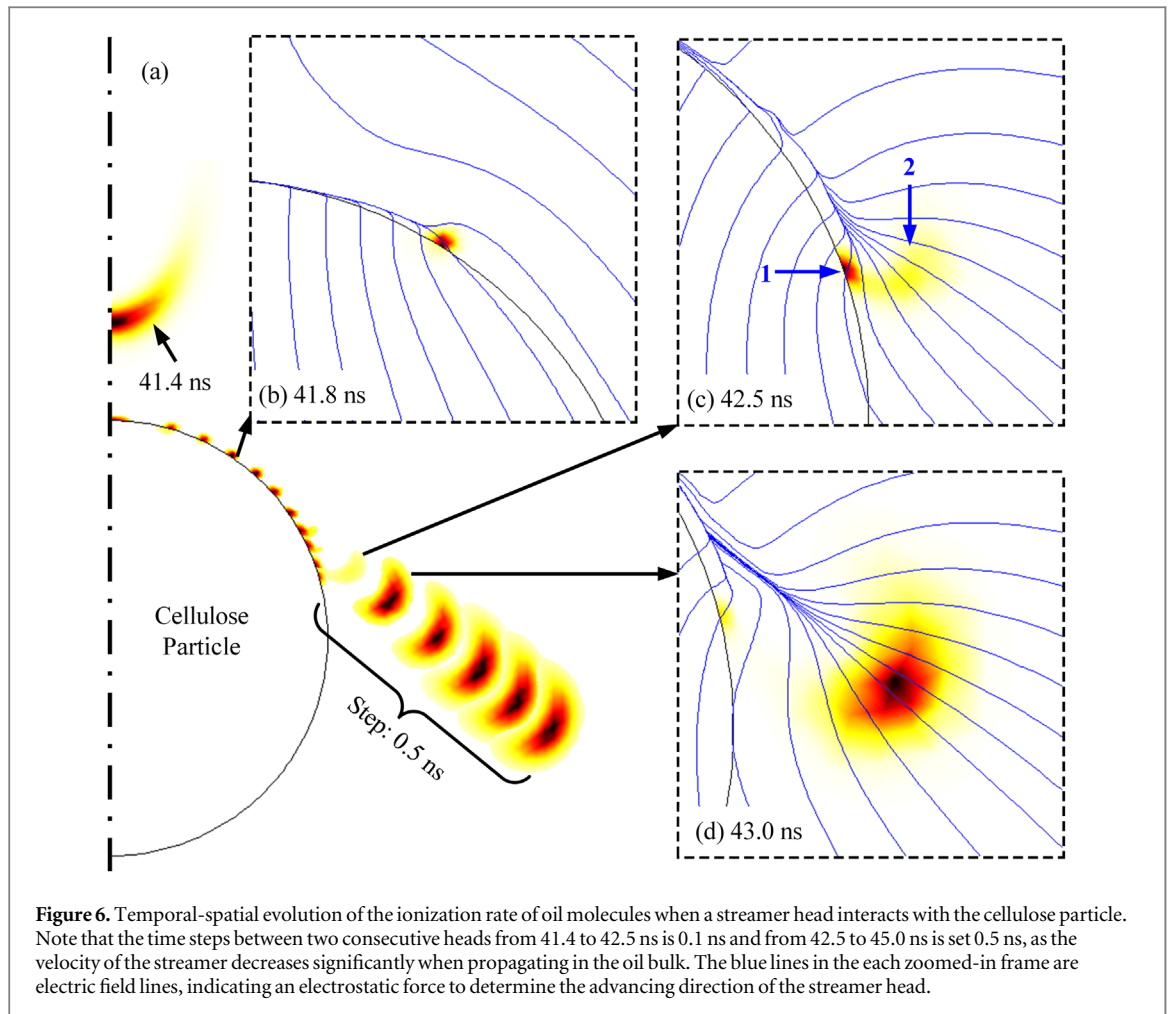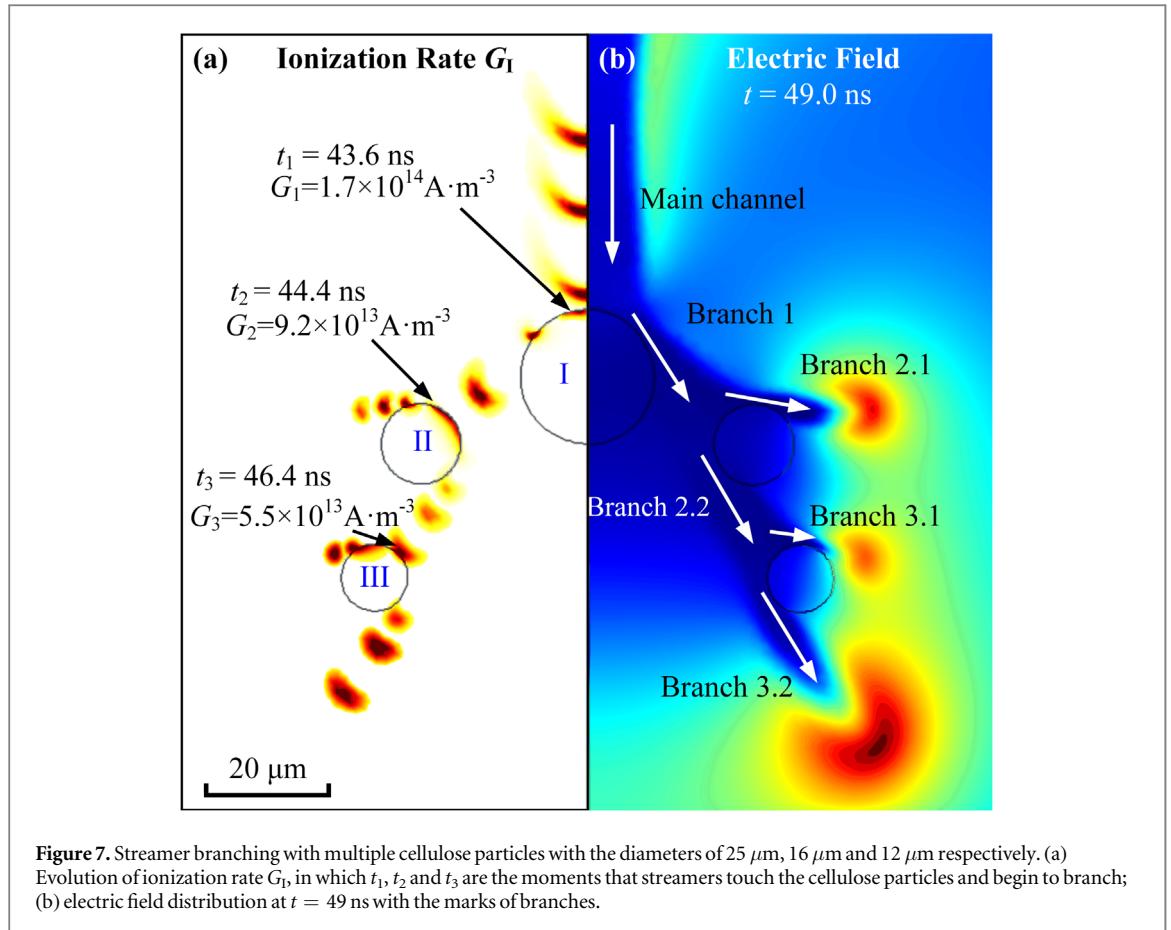
Figure 6. Temporal-spatial evolution of the ionization rate of oil molecules when a streamer head interacts with the cellulose particle. Note that the time steps between two consecutive heads from 41.4 to 42.5 ns is 0.1 ns and from 42.5 to 45.0 ns is set 0.5 ns, as the velocity of the streamer decreases significantly when propagating in the oil bulk. The blue lines in the each zoomed-in frame are electric field lines, indicating an electrostatic force to determine the advancing direction of the streamer head.

streamer head on the symmetric axis as 1.59×10^3 C·m^{-3} at 41.2 ns. The value climbs to 6.23×10^4 C·m^{-3} at the very beginning when the streamer head touches the particle surface at 41.6 ns. The zoomed frame of Panel 5b verifies that very high density of positive space charge forms in the thin layer along the local (narrow) surface and the diameters of the streamer (and the thickness of space charge layer) decrease after contacting the cellulose particle. However, the spherical particle disperses the charged particles on the surface area, hence reducing the space charge density from 41.8 ns to 42.0 ns as shown in Panels 5c and 5d. Although the streamer head has left the cellulose particle after 42.5 ns and the maximum space charge density reduces from 2.90×10^4 C·m^{-3} to 2.44×10^4 C·m^{-3}, the maximum space charge density still appears on the particle surface as the result of surface charge accumulation (see Panels 5e and 5f).

As described above in section 2, the generation and propagation of streamer are mainly driven by the direct ionization of oil molecules, i.e. Zener breakdown, in which the ionization rate (G_I) of the oil molecules is a function of electric field. Different from nephograms of the electric field and space charge presented above, the ionization rate of the oil molecules is a direct indicator to show the trajectory of the streamer head since G_I has a nonlinear relation with E as given by equation (5), and may be more sensitive to a slight change of E when the electric field exceeds certain threshold.

We plot the temporal-spatial evolution of G_I and electric field lines (E-lines) in figure 6 to describe a complete process of streamer propagating and interacting with the cellulose particle. Especially note that the evolution of G_I with time can be analogous to stroboscopic images by a train of short exposures of ICCD camera in experimental observations [33]. In this way, the advancing route of the propagating streamer heads and the process that a parent branch splits into two daughter branches are clearly recorded.

Strong ionization occurs along the surface between $t = 41.5$ ns and 42.5 ns due to the electric field enhancement on the interface. Before 42.5 ns, most of the electric field lines point into the cellulose particle (see Panel 6b), and positively charged particles are accumulated in a small region, forming a thin channel above the interface. The electric field lines start to scatter outwards of cellulose at 42.5 ns (Panel 6c), indicating an electrostatic force to drag the streamer head away from the surface and thereby into the oil bulk. Therefore, a streamer head can be split into two parts: one part is still adhesive to the cellulose surface (see 1 in Panel 6c) and the other moves into the bulk oil (see 2 in Panel 6c).

Figure 7. Streamer branching with multiple cellulose particles with the diameters of 25 μm, 16 μm and 12 μm respectively. (a) Evolution of ionization rate G_I, in which t_1, t_2 and t_3 are the moments that streamers touch the cellulose particles and begin to branch; (b) electric field distribution at $t = 49$ ns with the marks of branches.
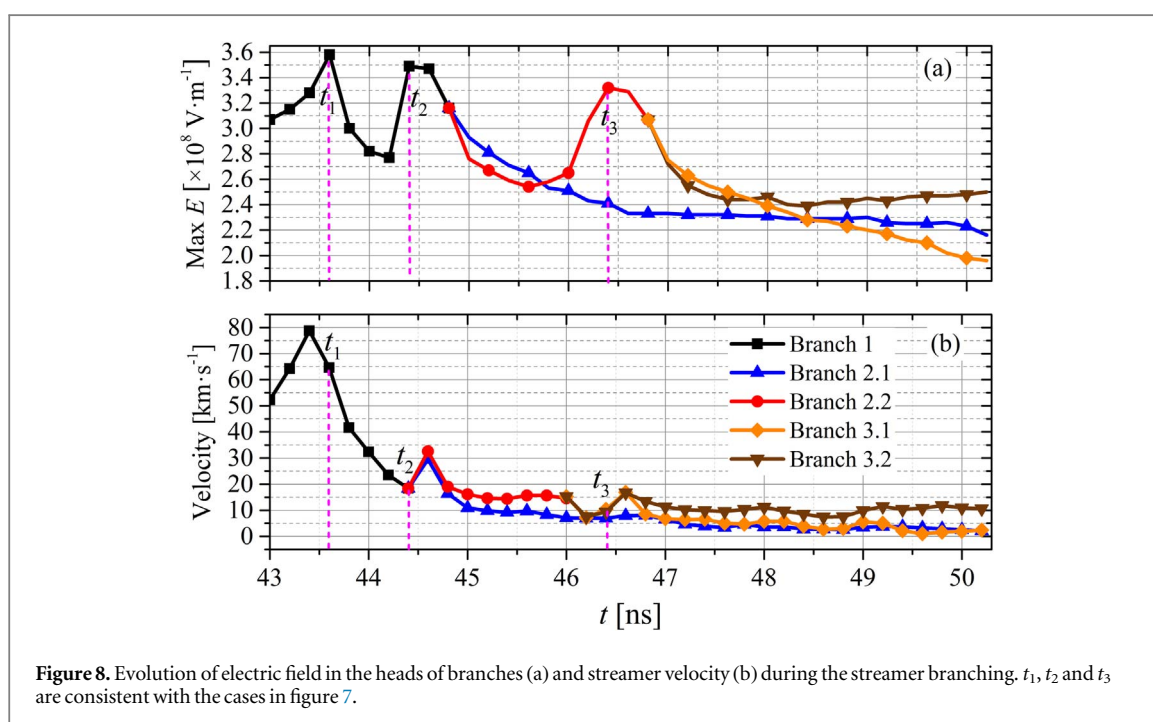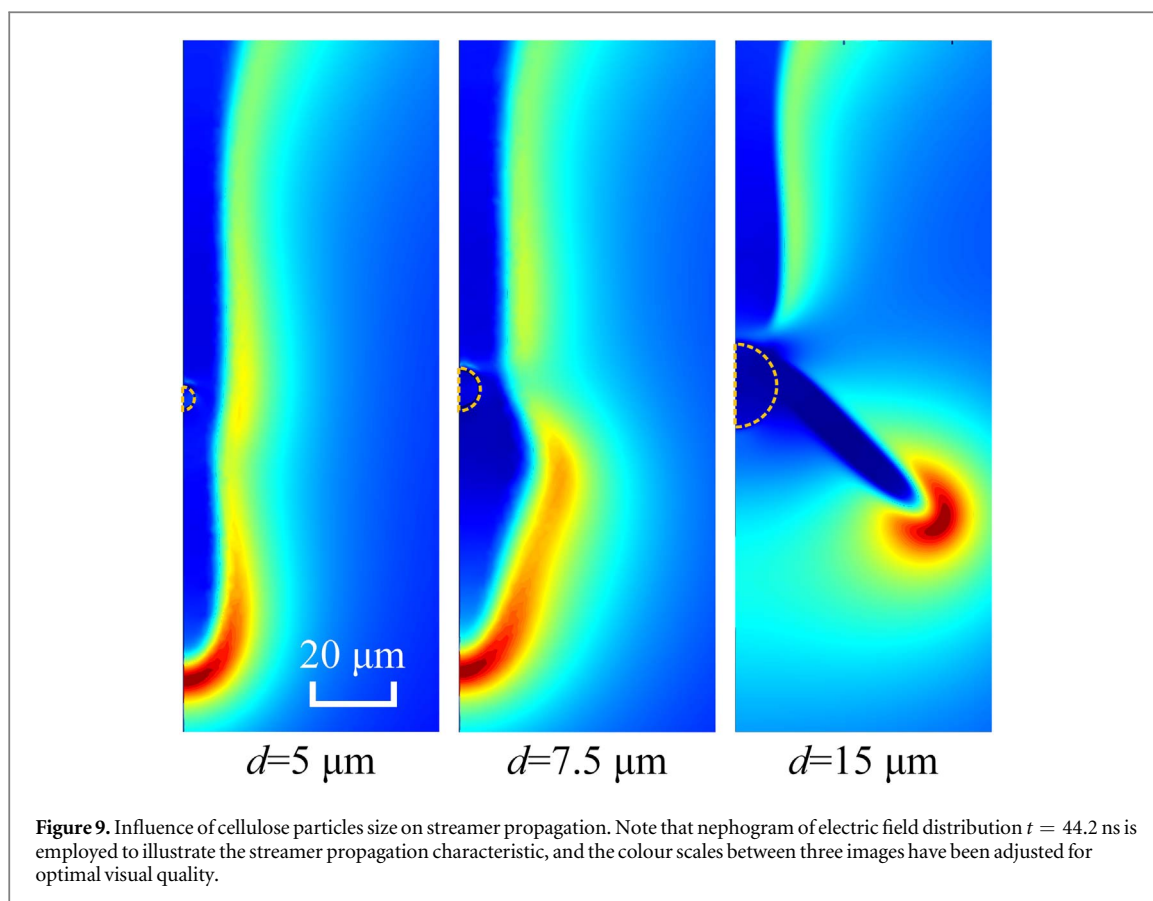
However, when multiple streamer heads are formed in the vicinity, the transportation route of electrons become complex and the interactions between two streamer heads are of importance in determining the branching behaviors. According to Panel 6c, when the streamer head 2 propagates forward into the oil, the electrons generated at the streamer head go back along E-lines to the anode. A portion of these fast moving electrons will neutralize positive ions within the streamer head 1, hence a decrease of the space charge density at the streamer head 1. Therefore, the electric field at the streamer head 1 decreases dramatically and the streamer dies out due to the lack of sufficient electric field to sustain the ionization and propagation (see Panel 6d). Streamer head 2 in the oil bulk can sustain a continuous ionization and propagates.
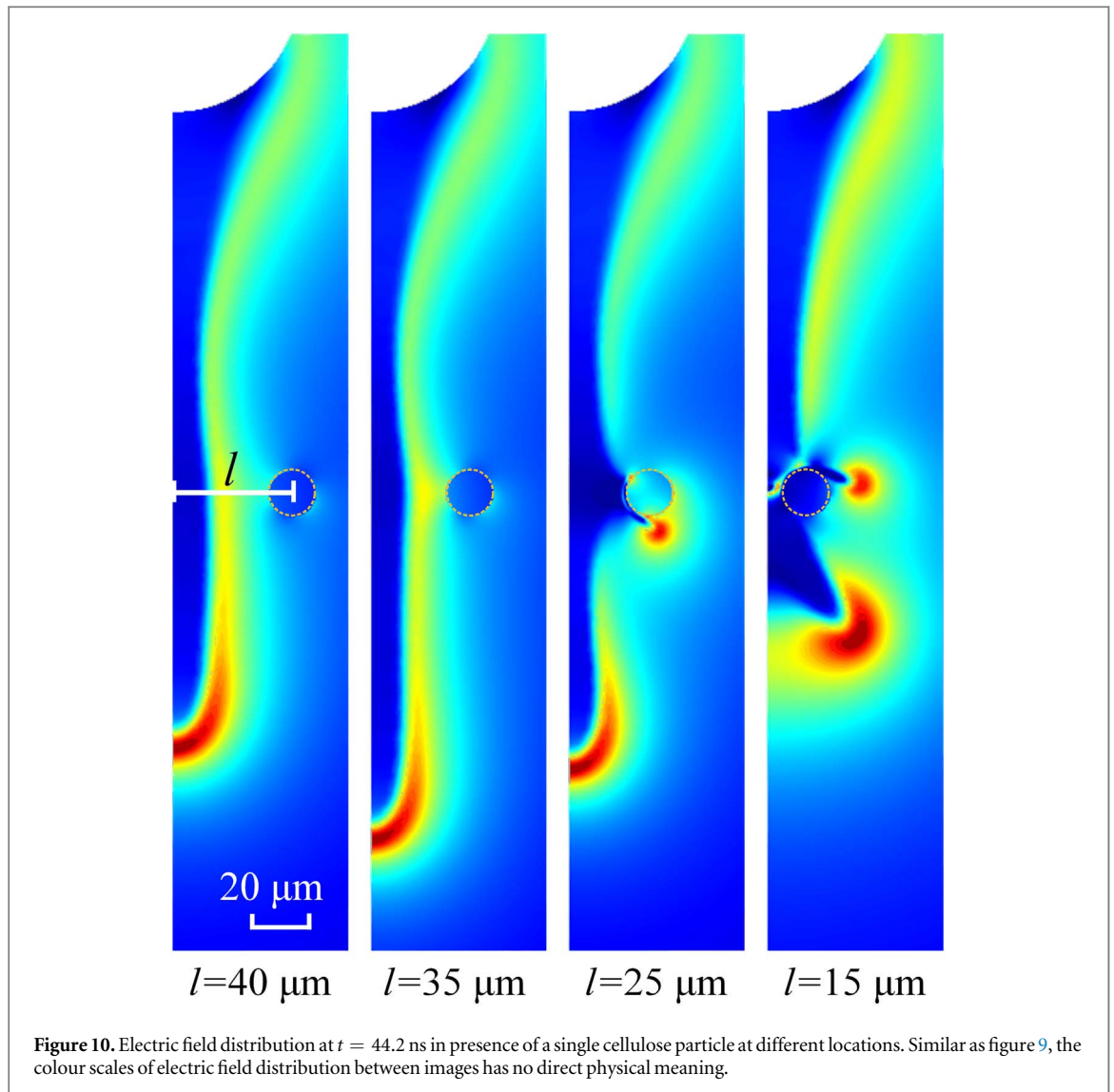
3.2. Multiple cellulose particles

A more practical situation is that a propagating streamer encounters with multiple impurities suspended in oil. In order to reveal the influences of multiple particles on streamer propagating and branching in oil, we have performed modelling incorporating three cellulose particles (axial symmetry). If all the scale of particles is relative large compared to the diameter of steamer, the branches will take too much time creeping on the surface of the particle. In this situation, the branching progress will be difficult to study or even do not happen in our simulation time scale ($\sim$70 ns). Therefore, to concentrate on the physical mechanism of branching, we select the diameters of three cellulose particles as 25 μm, 16 μm and 12 μm respectively. The cellulose particle with the diameter of 25 μm is centered on the z axis at (0, 0.975) with a distance of 125 μm from the anode tip. The cellulose particles with the diameter of 25 μm and 12 μm are centered at (0.035, 0.960) and (0.045, 0.935) respectively (all the coordinates are consistent with figure 1).

Figure 7 incorporates the evolution of ionization rate G_I with time and the electric field distribution at $t = 49$ ns under the condition of three cellulose particles on the route of streamer propagation. According to Panel 7a, the streamer reaches the surface of the cellulose particle I at 43.6 ns and split into two new streamers (considering the symmetric axis). We name Branch 1, Branch 2 and Branch 3 to identify their inherited relations that a parent branch splits into two daughter branches (e.g. Branch 2.2 is divided into branches 3.1 and 3.2). Temporally, Branch 1 splits at $t_2 = 44.4$ ns when hitting the cellulose particle II and Branch 2.2 splits at $t_3 = 46.4$ ns on the surface of particle III. The distribution of electric field at $t = 49$ ns (see figure 7(b)) is a complement to figure 7(a) indicating branching characteristics and possible quenching of the daughter branches, e.g. Branch 3.1.

Figure 9. Influence of cellulose particles size on streamer propagation. Note that nephogram of electric field distribution $t = 44.2$ ns is employed to illustrate the streamer propagation characteristic, and the colour scales between three images have been adjusted for optimal visual quality.

Figure 8. Evolution of electric field in the heads of branches (a) and streamer velocity (b) during the streamer branching. t_1, t_2 and t_3 are consistent with the cases in figure 7.

We extract the local maximum electric field at the streamer heads of branches and calculate the instantaneous propagation velocity of the branches, as illustrated in figure 8. It can be seen that when the heads of streamer contact with the surface of the cellulose particle, the local electric field increases sharply, hence the rise of ionization rate. Quantitatively, when the streamer heads touch the cellulose particles, the maximum electric field at the streamer head are 3.58×10^8 V·m^{-1}, 3.49×10^8 V·m^{-1}, and 3.32×10^8 V·m^{-1} respectively at t_1, t_2 and t_3. It is worth a mention, however, that the maximum electric field with time is decreasing in general. This is not only because the branches substantially disperse the charged particles on the cellulose surface and on

Figure 10. Electric field distribution at $t = 44.2$ ns in presence of a single cellulose particle at different locations. Similar as figure 9, the colour scales of electric field distribution between images has no direct physical meaning.

their propagating routes at different directions (in space), but also due to the branches deviating from the symmetric axis where the maximum Laplacian field locates.

Our previous simulation results of ideal transformer oil (without consideration of impurities like cellulose particles) [42] show that the velocity of streamer is mainly determined by the local electric field in front of the streamer head. However, it is surprisingly found from figure 8 that the peaks of the electric field and velocity do not occur synchronously when streamer interacting with the cellulose surface. The electric field is locally enhanced on the dielectric surface but streamer head is forced to change the propagating direction in the presence of the cellulose particle. Although the ionization of oil molecules along the cellulose surface is strong, the massive charged particles require some time accumulating to form new heads. A decrease of the propagating velocity is thereby observed. Therefore, the local electric field is not the only decisive factor influencing the propagating velocity of streamer in presence of barrier dielectrics.

When the streamer heads leave the cellulose particle, not all the branches can maintain self-sustaining development to approach the cathode electrode. In fact, most of the branches tend to extinguish and commonly only one of the branches could continue to propagate further (see Branch 2.1, 3.1 and 3.2 in figure 7). The interaction of multiple streamer branches taking homogenously positive charges uniforms the local electric field, but the electric field ahead of Branch 3.2 is slightly enhanced. This can be verified by the fact that the electric field at the head of Branch 3.2 increases from 2.4×10^{8} V·m^{-1} to 2.5×10^{8} V·m^{-1} during 48 to 50 ns (see figure 8(b)), while other branches have a decaying electric field and ceased propagation.

3.3. Particle size and location

It can be speculated, from above simulation results, that the size and suspending location of cellulose particles play a very significant role in the propagation and branching of streamer in transformer oil. The industrial

community commonly divides the particle in the transformer oil into three classes by size in diameter d: $d > 4$ μm, $d > 6$ μm and $d > 14$ μm (IEC 60970: 2007 [49]). In this part, the influences of the particle size and location on the streamer propagation are investigated. Three kinds of cellulose particles of varying diameters, $d = 5$ μm, 7.5 μm, 15 μm are selected in the simulation. The centre of each particle is set on the symmetric axis, 125 μm away from the pointed anode electrode.

The influence of three kinds of cellulose particles on streamer propagation electric field distributions are shown in figure 9. In our simulation, the diameters of streamers in transformer oil are estimated around 40 μm. When d is below 5 μm, the particle is too small to have any pronounced impact on the streamer propagation. The streamer envelopes the cellulose particle and continues to elongate along the symmetric axis with a slightly decreased diameter. When the diameter of the cellulose particle grows to 7.5 μm, it will take longer time for streamer to creep along the particle surface than the case of 5 μm, but the streamer channel will have more likelihood to expand. After the streamer passes the particle under both situations, the streamer channel does not branch and will restore to original width (e.g. when $t > 45$ ns). However, when the diameter of cellulose particle is 15 μm that the particle size is comparable to the streamer diameter, the electric field on the dielectric surface shares more horizontal component leading the streamer channel to travel outwards. Branching occurs and the discharge channel splits into two streamer heads.

On the particle location, we set each cellulose particle of 10 μm in diameter moving on the horizontal line that is 125 μm away from the point electrode. We adjust the direct distance from the centre of the cellulose particle to the symmetric axis, $l = 40$ μm, 35 μm, 25 μm, 15 μm, to investigate that how far a cellulose particle sits can influence a streamer. The electric field distribution at $t = 44.2$ ns in presence of a single cellulose particle at different locations is shown in figure 10.

When l is no less than 35 μm, the advancing direction of streamer is not influenced by the cellulose particle, while the propagating velocity increases when the particle sits closer (compare the cases $l = 40$ μm and 35 μm, the later streamer moves further), due to the local enhancement of electric field related to the cellulose particle with high permittivity. When l is less than 25 μm that the particle is very close to the advancing route of the streamer, the branching probability increases. The distinction is that the main channel of the streamer in the case of $l = 25$ μm still propagates along the symmetric axis, while a protrusion on the side of the streamer grows, which finally develops into a tiny branch. When the particle is on the route of discharge channel ($l = 15$ μm), streamer entirely creeps on the cellulose particle and the velocity of streamer decreases dramatically. In this case, more than four branches are observed and the main advancing direction is deviated from the symmetric axis (considering the axial symmetry).

4. Summary and conclusion

In this work, we investigate the influence of microscopic dielectric impurities, i.e. cellulose particles, on the streamer propagation and branching in transformer oil by modelling approach. The number of cellulose particles (single and three particles), their size and locations are key variables elucidating the influencing mechanisms.

The streamer interacting processes with a cellulose particle with diameter of 50 μm show that the maximum electric field increases dramatically to 6.85×10^8 V m^{-1} when the streamer channel approaches the particle surface. At the same time, the instant propagating velocity rises to 84.1 km s^{-1} and the maximum space charge density climbs to 6.23×10^4 C·m^{-3}. However, the spherical particle acts as a barrier and disperses the charged particles on the surface area, hence reducing the propagating velocity and the space charge density later. The distribution of the electric field along the symmetric axis of spherical surface of cellulose quantitatively show that a thin plasma layer ($\sim$5 μm) propagates along the surface and the electric field clearly decreases to 2.5×10^8 V·m^{-1} when the streamer head leaves the surface. The ionization rate (G_I) of the oil molecules indicates that the interactions between the two heads allow one head to continuously propagate, while the other dies out due to insufficient ionization rate.

When encountered with multiple cellulose particles, a streamer will experience several times of branching events. The maximum electric field and velocity of the streamer heads do not occur synchronously when streamer interacting with the cellulose surfaces. The electric field is locally enhanced on the dielectric surface but streamer head is forced to change the propagating direction in the presence of the cellulose particle, hence a decrease of the propagating velocity. The simulation results indicate that most of the branches tend to extinguish and commonly only one branch could competitively survive to propagate further.

Our modelling results show that the size and suspending location of cellulose particles can substantially affect the propagation and branching of streamer in transformer oil. When the particle is too small, it will have no pronounced impact on the streamer propagation. However, when the particle size is comparable to the streamer diameter, the electric field on the dielectric surface shares more horizontal component causing the

branching. Placing the particle very close to or on the route of discharge channel will cause that the streamer creeps on the cellulose particle and the velocity of streamer decreases dramatically, then more branches are observed.

It is worth pointing out that the presented model and results analysis concentrate on the streamer initiation and interactions of streamer head on the interface of liquid-solid dielectrics, the streamer plasma inside the discharge channels are not highlighted in this study. However, the multi-phase interactions (liquid-gas-solid) are of great physical significance but have many difficulties so far. One of main problems is that transformer oil is comprised of numerous individual molecular species, while the classic transportation parameters of liquid molecules like electron mobility, ion recombination rate, and molecular ionization energy are not well known. Incorporating interdisciplinary knowledge, for instance quantum chemistry, like density functional theory, may provide solutions to more accurate estimation of field-dependent ionization potential [43]. Besides, the vaporization process caused by Joule heating inside the streamer channel may also influence the propagation and branching of streamer. Thus for a more proper approximation, the phase transitions during the streamer propagation should be included in the near future.

Acknowledgments

ORCID iDs

Yuan Li ⓘ https://orcid.org/0000-0001-5424-1764
Jiaye Wen ⓘ https://orcid.org/0000-0001-8160-5148

References

[1] Danikas M G 1990 Breakdown of transformer oil *IEEE Electr. Insul. Mag.* **6** 27–34
[2] Pontiga F and Castellanos A 1996 The effect of field-enhanced injection and dissociation on the conduction of highly-insulating liquids *IEEE Trans. Dielectr. Electr. Insul.* **3** 792–9
[3] Joshi R P, Kolb J F, Xiao S and Schoenbach K H 2009 Aspects of plasma in water: streamer physics and applications *Plasma Processes Polym.* **6** 763–77
[4] Paul D and Goswami A K 2019 Copula based bivariate modelling of DGA and breakdown voltage in high voltage transformers and reactors *IEEE Trans. Dielectr. Electr. Insul.* **26** 1763–70
[5] Tang C, Chen G, Fu M and Liao R 2010 Space charge behavior in multi-layer oil-paper insulation under different DC voltages and temperatures *IEEE Trans. Dielectr. Electr. Insul.* **17** 775–84
[6] Liu Q and Wang Z 2011 Streamer characteristic and breakdown in synthetic and natural ester transformer liquids under standard lightning impulse voltage *IEEE Trans. Dielectr. Electr. Insul.* **18** 285–94
[7] Hebner R E 1988 Measurement of electrical breakdown in liquids *The Liquid State and Its Electrical Properties* ed E E Kunhardt *et al* (Boston, MA: Springer US) vol 193, pp 519–37
[8] Luque A, González M and Gordillo-Vázquez F J 2017 Streamer discharges as advancing imperfect conductors: inhomogeneities in long ionized channels *Plasma Sources Sci. Technol.* **26** 125006
[9] Rouse T O 1998 Mineral insulating oil in transformers *IEEE Electr. Insul. Mag.* **14** 6–16
[10] Adamovich I *et al* 2017 The 2017 Plasma Roadmap: low temperature plasma science and technology *J. Phys. D: Appl. Phys.* **50** 323001
[11] Arrayas M, Ebert U and Hundsdorfer W 2002 Spontaneous branching of anode-directed streamers between planar electrodes *Phys. Rev. Lett.* **88** 174502
[12] Vanraes P and Bogaerts A 2018 Plasma physics of liquids—A focused review *Appl. Phys. Rev.* **5** 031103
[13] Luque A and Ebert U 2011 Electron density fluctuations accelerate the branching of streamer discharges in air *Phys. Rev.* E **84** 046411
[14] Shen S, Liu Q and Wang Z 2019 Effect of electric field uniformity on positive streamer and breakdown characteristics of transformer liquids *IEEE Trans. Dielectr. Electr. Insul.* **26** 1814–22
[15] Lesaint O 2016 Prebreakdown phenomena in liquids: propagation 'modes' and basic physical properties *J. Phys. D: Appl. Phys.* **49** 144001
[16] Lesaint O and Massala G 1998 Positive streamer propagation in large oil gaps: experimental characterization of propagation modes *IEEE Trans. Dielectr. Electr. Insul.* **5** 360–70
[17] Rocco A, Ebert U and Hundsdorfer W 2002 Branching of negative streamers in free flight *Phys. Rev.* E **66** 035102
[18] Hallac A, Georghiou G E and Metaxas A C 2005 Streamer branching in transient nonuniform short gap discharges using numerical modeling *IEEE Trans. Plasma Sci.* **33** 266–7
[19] Teunissen J and Ebert U 2017 Simulating streamer discharges in 3D with the parallel adaptive Afivo framework *J. Phys. D: Appl. Phys.* **50** 474001
[20] Madshaven I, Hestad O, Unge M, Hjortstam O and Åstrand P 2019 Conductivity and capacitance of streamers in avalanche model for streamer propagation in dielectric liquids *Plasma Research Express* **1** 035014
[21] Devins J C, Rzad S J and Schwabe R J 1981 Breakdown and prebreakdown phenomena in liquids *J. Appl. Phys.* **52** 4531–45
[22] Devins J C, Rzad S J and Schwabe R J 1976 Prebreakdown phenomena in liquids: electronic processes *J. Phys. D: Appl. Phys.* **9** L87–91
[23] Zener C 1934 A theory of the electrical breakdown of solid dielectrics *Proceedings of the Royal Society A: Mathematical, Physical and Engineering Sciences* **145** 523–9

[24] Jadidian J, Zahn M, Lavesson N, Widlund O and Borg K 2013 Stochastic and deterministic causes of streamer branching in liquid dielectrics *J. Appl. Phys.* **114** 063301

[25] Hwang J G, Zahn M and Pettersson L A A 2012 Mechanisms behind positive streamers and their distinct propagation modes in transformer oil *IEEE Trans. Dielectr. Electr. Insul.* **19** 162–74

[26] Aljure M, Becerra M and Karlsson M E 2019 On the injection and generation of charge carriers in mineral oil under high electric fields *J. Phys. Commun.* **3** 035019

[27] Becerra M, Aljure M and Nilsson J 2019 Assessing the production and loss of electrons from conduction currents in mineral oil *2019 IEEE 20th Int. Conf. on Dielectric Liquids (ICDL)* (Roma, Italy: IEEE) pp 1–4

[28] Bruggeman P J *et al* 2016 Plasma–liquid interactions: a review and roadmap *Plasma Sources Sci. Technol.* **25** 053002

[29] Madshaven I, Hestad O, Unge M, Hjortstam O and Åstrand P 2020 Photoionization model for streamer propagation mode change in simulation model for streamers in dielectric liquids *Plasma Research Express* **2** 015002

[30] Oladiran E O 1982 On the propagation of streamers through a large population of neutral droplets *Pure and Applied Geophysics PAGEOPH* **120** 673–81

[31] GIGRE Working Group 12.17 2000 *Effect of Particles on Transformer Dielectric Strength* CIGRE Technical Brochure 157

[32] Tardiveau P and Marode E 2003 Point-to-plane discharge dynamics in the presence of dielectric droplets *J. Phys. D: Appl. Phys.* **36** 1204–11

[33] Oladiran E O 1981 The interaction of positive streamers with charged and uncharged water drops in vertical electric fields *Pure and Applied Geophysics PAGEOPH* **119** 966–77

[34] Sigmond R S, Sigmond T, Rolfseng L, Bohman A F, Stormo F-T and Hvidsten L 2004 The Aiming of the Bolt: How a Flashover Finds the Weak Spot *IEEE Trans. Plasma Sci.* **32** 1812–8

[35] Akishev Y, Arefi-Khonsari F, Demir A, Grushin M, Karalnik V, Petryakov A and Trushkin N 2015 The interaction of positive streamers with bubbles floating on a liquid surface *Plasma Sources Sci. Technol.* **24** 065021

[36] Dung N V, Hoidalen H K, Linhjell D, Lundgaard L E and Unge M 2012 Influence of impurities and additives on positive streamers in paraffinic model oil *IEEE Trans. Dielectr. Electr. Insul.* **19** 1593–603

[37] Lu X and Ostrikov K (Ken) 2018 Guided ionization waves: the physics of repeatability *Appl. Phys. Rev.* **5** 031102

[38] Aka-Ngnui T and Beroual A 2001 Modelling of multi-channel streamers propagation in liquid dielectrics using the computation electrical network *J. Phys. D: Appl. Phys.* **34** 794–805

[39] Fowler H A, Devaney J E and Hagedorn J G 2003 Growth model for filamentary streamers in an ambient field *IEEE Trans. Dielectr. Electr. Insul.* **10** 73–9

[40] Babaeva N Y, Tereshonok D V, Naidis G V and Smirnov B M 2016 Streamer branching on clusters of solid particles in air and air bubbles in liquids *J. Phys. Conf. Ser.* **774** 012151

[41] Li Y, Mu H-B, Wei Y-H, Zhang G-J, Wang S-H, Zhang W-Z, Li Z-M, Jadidian J and Zahn M 2014 Sub-microsecond streamer breakdown in transformer oil-filled short gaps *IEEE Trans. Dielectr. Electr. Insul.* **21** 1616–26

[42] Li Y, Zhu M X, Mu H B, Deng J B, Zhang G J, Jadidian J, Zahn M, Zhang W Z and Li Z M 2014 Transformer oil breakdown dynamics stressed by fast impulse voltages: experimental and modeling investigation *IEEE Trans. Plasma Sci.* **42** 3004–13

[43] Davari N, Åstrand P-O and Van Voorhis T 2013 Field-dependent ionisation potential by constrained density functional theory *Mol. Phys.* **111** 1456–61

[44] Ariza D, Becerra M, Hollertz R, Wagberg L and Pitois C 2017 First mode negative streamers along mineral oil-solid interfaces *IEEE Trans. Dielectr. Electr. Insul.* **24** 2371–82

[45] Ghassemi M, Tefferi M B, Chen Q and Cao Y 2017 A thermo-electrodynamic electric field dependent molecular ionization model to realize positive streamer propagation in a wet-mate DC connector *IEEE Trans. Dielectr. Electr. Insul.* **24** 901–14

[46] Naidis G V 2015 Modeling of subnanosecond discharge in hydrocarbon liquid *IEEE Trans. Plasma Sci.* **43** 3138–41

[47] Lietz A M, Damany X, Robert E, Pouvesle J-M and Kushner M J 2019 Ionization wave propagation in an atmospheric pressure plasma multi-jet *Plasma Sources Sci. Technol.* **28** 125009

[48] Zhang C, Huang B, Luo Z, Che X, Yan P and Shao T 2019 Atmospheric-pressure pulsed plasma actuators for flow control: shock wave and vortex characteristics *Plasma Sources Sci. Technol.* **28** 064001

[49] International Electrotechnical Comission 2007 IEC 60970 Insulating liquids—Methods for counting and sizing particles